JOURNAL OF SOLID STATE CHEMISTRY 93, 395–402 (1991)

Electrical Conductivities of $YBa_2M_3O_y$ (M: Fe, Co) System

YASUMICHI MATSUMOTO AND JUKICHI HOMBO

Department of Applied Chemistry, Faculty of Engineering, Kumamoto University, Kurokami 2-39-1, Kumamoto, Japan 860

Received November 5, 1990; in revised form March 28, 1991

$YBa_2M_3O_{9-\delta}$ (M: Fe, Co) systems with composition similar to the $YBa_2Cu_3O_7$ superconductor were synthesized. Two types of $Y_{1.2}Ba_3Fe_3O_z$ (orthorhombic, $a = b = 4.06$ Å, $c = 4.04$ Å) and $YBa_2Fe_3O_{9-\delta}$ (tetragonal, $a = 3.94$ Å, $b = 3.92$ Å, $c = 3.90$ Å) with perovskite-type structure were obtained for the iron oxide system, while $YBa_2Co_3O_{9-\delta}$ perovskite (cubic, $a = 4.14$ Å) was obtained for the cobalt oxide system. The conductivities and the Seebeck coefficients were measured in the temperature range from 650°C to room temperature. The carrier densities and the mobilities were calculated by using a small polaron hopping model. All the samples were p-type semiconductors and showed hopping conduction. The mobility of holes was much larger for $YBa_2Co_3O_{9-\delta}$ than for $YBa_2Fe_3O_{9-\delta}$, although the unit cell is larger for the former oxide than for the latter. This is explained through the larger overlapping integral of the σ^* hopping band formed in $YBa_2Co_3O_{9-\delta}$ than the π^* hopping band formed in $YBa_2Fe_3O_{9-\delta}$.

Introduction

It is well known that $YBa_2Cu_3O_{7-\delta}$ is a high-T_c superconductor with perovskite like structure. Partial substitutions of many kinds of metals for Cu in this oxide were carried out for the purpose of improving superconducting properties, but no improvement has been found. Co and Fe can be easily substituted for Cu, although the critical temperature shifts to much lower than 90 K by these substitutions (*1–4*). This suggests that oxides completely substituted by Co and Fe for Cu, i.e., $YBa_2M_3O_y$ (M: Co, Fe) can be easily prepared. Studying the electrical conductivities of these oxides seems to be very important for the elucidation of contribution of Cu ion to the superconduction. $Y(Ba,K)_2Co_3O_y$, which has a structure similar to $YBa_2Cu_3O_{7-\delta}$, has been synthesized already, and is a semiconductor (*5*). However, single phases of $YBa_2Co_3O_y$ and $YBa_2Fe_3O_y$ have not been prepared until now.

We have found that the electrical conductivities of iron and cobalt perovskite oxides are based on the hopping mechanism, and that the carrier mobility depends on the M–O–M distance and the amount of oxygen vacancy in the structure (*6*). Since it can be expected for $YBa_2M_3O_y$ to have perovskite-type structure, their conductivities will also be controlled by the hopping mechanism. In this paper, we report on the synthesis of $YBa_2M_3O_y$(M: Fe, Co) and their electrical conductivities and discuss the difference between their conduction mechanisms.

Experimental

Fe_2O_3, Co_2O_3, $BaCO_3$, and Y_2O_3 were used as the starting materials for the prepa-

0022-4596/91 $3.00

rations of $YBa_2M_3O_y$(M: Co, Fe). The stoichiometrical mixtures were heated at 1100°C for several hours in air. The samples were reground and then pressed into a tablet (1600 kg/cm^2), followed by sintering at 1100°C for 7 hr in air. The crystal structures of the sintered samples were analyzed by an X-ray diffraction method. The structure of all the samples were perovskite type, i.e., it differed from the $YBa_2Cu_3O_{7-\delta}$ superconductor in structure. However, various annealings were necessary for the preparation of a single phase of perovskite, as stated in a later section. The thermogravimetric analysis (TG) was carried out in O_2, air, and N_2 in order to determine the oxygen vacancy in the oxides. The conductivities were measured by the four-probe method using Ag leads under a constant current of 0.01 mA. The conductivities and the Seebeck coefficients of the samples, whose sizes was 8 × 4 mm and thickness was 2 mm, were measured in the temperature range from 650°C to room temperature. The temperature difference between both edges of the sample was kept at 4–6°C for the case of the measurement of the Seebeck coefficient. All the measurements were carried out under a slow cooling rate (about 1°C/min) after heating for 1 hr at 650°C in each atmosphere.

Results and Discussion

$YBa_2Fe_3O_{9-\delta}$ Perovskite

Figure 1 shows the X-ray diffraction patterns of $YBa_2Fe_3O_{9-\delta}$. An as-grown sample sintered at 1100°C in air (A in Fig. 1) was a mixture of perovskite (orthorhombic, $a = b = 4.06$ Å, $c = 4.04$ Å), $BaFe_2O_4$, $YFeO_3$, and Y_2O_3. The composition of this perovskite phase was determined to be $Y_{1.2}Ba_3Fe_3O_z$ by EDX analysis. The unit cell of this perovskite is close to that of $BaFeO_{3-\delta}$ ($a = 4.01$ Å) in size, suggesting that the Ba ion rather than the Y ion contributes importantly to the formation of perovskite structure. Some of the excess Y ion in $Y_{1.2}Ba_3Fe_3O_z$ perovskite will exist in the Fe site and the other will exist in the Ba site in its structure. The single phase of perovskite (tetragonal, $a = 3.94$ Å, $b = 3.92$ Å, $c = 3.90$ Å) was obtained by heat treatment of the above sample at 1100°C in N_2 (B in Fig. 1). The formation of a single phase of perovskite and the decrease in the unit cell by annealing in N_2 is based on the release of Ba ions from the $Y_{1.2}Ba_3Fe_3O_z$ perovskite phase together with the production of an oxygen vacancy. However, we could never prepare the oxide with the same structure as $YBa_2Cu_3O_{7-\delta}$. Probably, it will be very difficult that the Fe ion is situated at a square planar or a pyramidal coordination site in the oxide such as $YBa_2Cu_3O_{7-\delta}$.

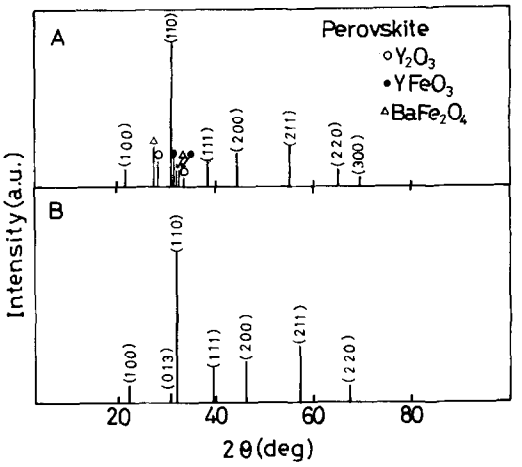

FIG. 1. X-ray diffraction patterns of Y–Ba–Fe oxide system: (A) as-grown sample sintered at 1100°C in air, (B) heat-treated sample (A) at 1100°C in N_2.

From the following reaction and the TG measurements, the oxygen vacancy concentration δ in $YBa_2Fe_3O_{9-\delta}$ annealed in N_2 was determined to be 1.15 at room temperature

$$\tfrac{1}{2}Y_2O_3 + 2BaCO_3 + \tfrac{3}{2}Fe_2O_3 \xrightarrow{1100°C,\ air} Y_{1.2}Ba_3Fe_3O_z, BaFe_2O_4, Y_2O_3, YFeO_3 \xrightarrow{1100°C,\ N_2} YBa_2Fe_3O_{9-\delta} \quad (1)$$

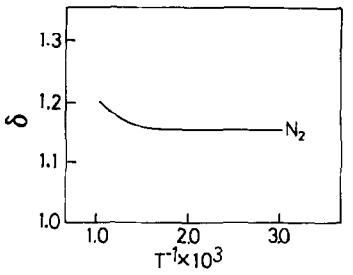

FIG. 2. δ in $YBa_2Fe_3O_{9-\delta}$ as a function of temperature in N_2.

When $YBa_2Fe_3O_{9-\delta}$ was heated in air and O_2 at temperatures higher than about 650°C, $Y_{1.2}Ba_3Fe_3O_z$ was formed again. Figure 2 shows δ in $YBa_2Fe_3O_{9-\delta}$ calculated from the TG curve as a function of temperature. This measurement was done at a cooling rate of 1°C/min, which was enough for the sample to attain an equilibrium state in oxygen reaction, because the weight loss of the samples by the production of oxygen vacancies became immediately constant (<1 min) after keeping at various temperatures higher than about 250°C and no weight loss was observed at temperatures lower than this point. The increase of oxygen vacancy concentration at temperatures higher than about 300°C is based on the release of oxygen from the perovskite structure. This is a characteristic phenomenon for the oxides with perovskite-type structure, which has been already observed in other iron perovskites such as $BaFeO_{3-\delta}$ and $SrFeO_{3-\delta}$ (*6*).

The electrical measurements were done for $YBa_2Fe_3O_{9-\delta}$ and $Y_{1.2}Ba_3Fe_3O_z$, although the latter oxide had a small amount of Y_2O_3, $YFeO_3$, and $BaFe_2O_4$ as the impurities. Figure 3 shows conductivity, σ, and Seebeck coefficient, Q, as a function of temperature for $YBa_2Fe_3O_{9-\delta}$ in N_2. As seen, $YBa_2Fe_3O_{9-\delta}$ was a p-type semiconductor. From the conductivity and the Seebeck coefficient, hole density and mobility can be calculated by using a small polaron hopping model as represented by the equations

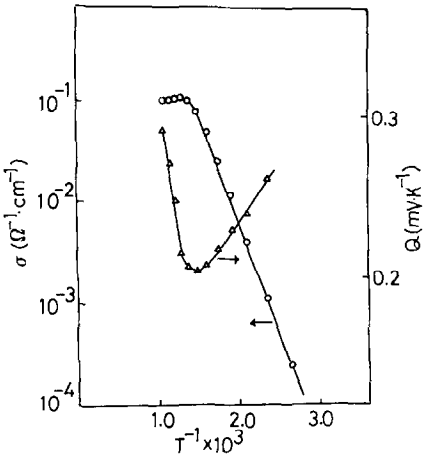

FIG. 3. Conductivity and Seebeck coefficient of $YBa_2Fe_3O_{9-\delta}$ as a function of temperature in N_2.

$$Q = -(k/e)\ln(n_1/n_2) \tag{2}$$

$$\sigma = e\mu P, \tag{3}$$

where n_1 and n_2 are the electron vacant and the electron occupied site numbers, respectively, which have been explained in detail in Ref. (*6*). P and μ are the majority carrier density and the mobility, respectively.

Figure 4 shows the hole density and the

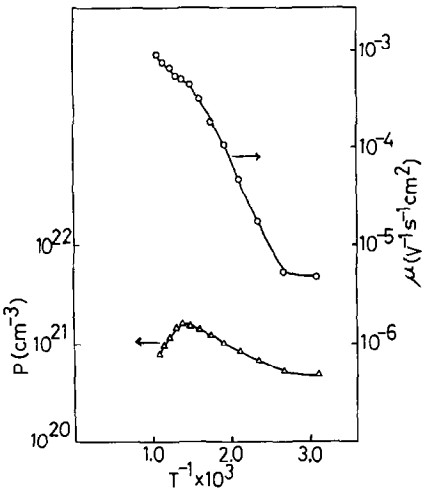

FIG. 4. Hole density and mobility of $YBa_2Fe_3O_{9-\delta}$ as a function of temperature in N_2.

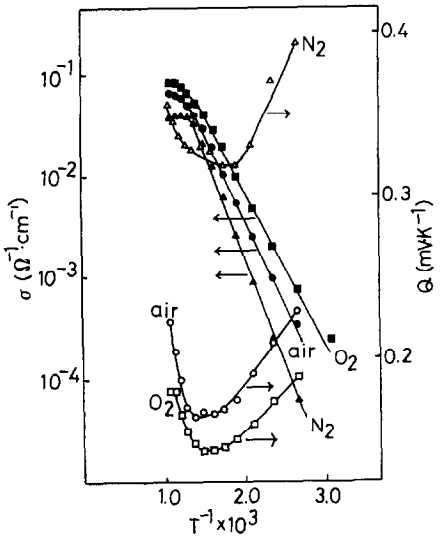

FIG. 5. Conductivity and Seebeck coefficient of $Y_{1.2}Ba_3Fe_3O_z$ as a function of temperature in O_2, air, and N_2.

mobility as a function of temperature. The mobility depends strongly on temperature, but not the hole density. This indicates that the conductivity of $YBa_2Fe_3O_{9-\delta}$ is determined by the hopping mechanism. The activation energy was 0.32 eV in the temperature range from 150 to 400°C. The small decrease in the hole density at temperatures higher than about 400°C is due to the production of an oxygen vacancy as shown in Fig. 2. These phenomena are similar to those of $BaFeO_{3-\delta}$ and $SrFeO_{3-\delta}$ (6).

We have also measured the electrical conductivities and the Seebeck coefficients of $Y_{1.2}Ba_3Fe_3O_z$ in O_2, air, and N_2, although these values may be relatively rough because of the presence of a small amount of the impurities stated above. This oxide was also a p-type semiconductor with conductivity and its activation energy was similar to those of $YBa_2Fe_3O_{9-\delta}$. Thus, the effect of impurity on the conductivity measured in this study was not very large. The conductivity and the Seebeck coefficient of this oxide as a function of temperature are shown in Fig. 5.

The oxide shows a typical p-type semiconductivity, that is, its conductivity decreases in N_2 and increases in O_2. The Seebeck coefficient showed that this oxide is also a p-type semiconductor. A strange phenomenon is that the conductivity of $YBa_2Fe_3O_{9-\delta}$ (Fig. 3) is higher than that of $Y_{1.2}Ba_3Fe_3O_z$ in N_2 and is about same as those in O_2 and air (Fig. 5). According to the same analysis using conductivity and Seebeck coefficient as stated above, the calculated mobility of $Y_{1.2}Ba_3Fe_3O_z$ is smaller than that of $YBa_2Fe_3O_{9-\delta}$ by about three times, as shown in Fig. 6. This is the main reason of the above phenomenon. The larger mobility of $YBa_2Fe_3O_{9-\delta}$ compared to that of $Y_{1.2}Ba_3Fe_3O_z$ is based on the distance of Fe–O–Fe being smaller for the former oxide (3.92–3.94 Å) than for the latter oxide (4.04–4.06 Å).

$YBa_2Co_3O_{9-\delta}$ Perovskite

Figure 7 shows the X-ray diffraction patterns of $YBa_2Co_3O_{9-\delta}$ samples produced by various heat treatments. The final product

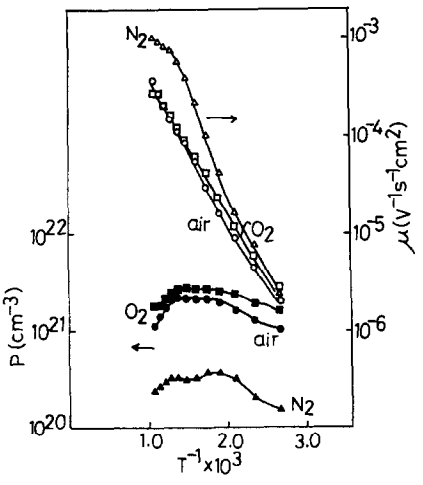

FIG. 6. Hole density and mobility of $Y_{1.2}Ba_3Fe_3O_z$ as a function of temperature in O_2, air, and N_2.

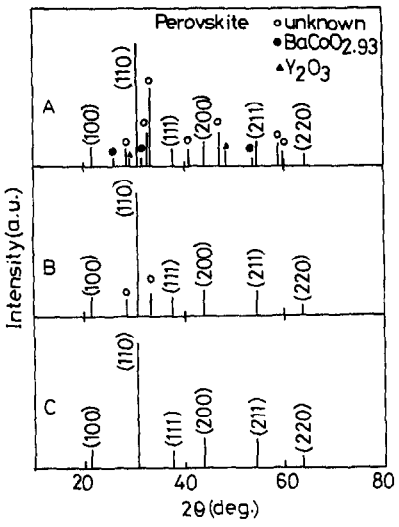

FIG. 7. X-ray diffraction patterns of Y–Ba–Co oxide system: (A) as-grown sample sintered at 1100°C in air, (B) heat-treated sample (A) at 1100°C in N_2, (C) heat-treated sample (B) at 650°C in O_2.

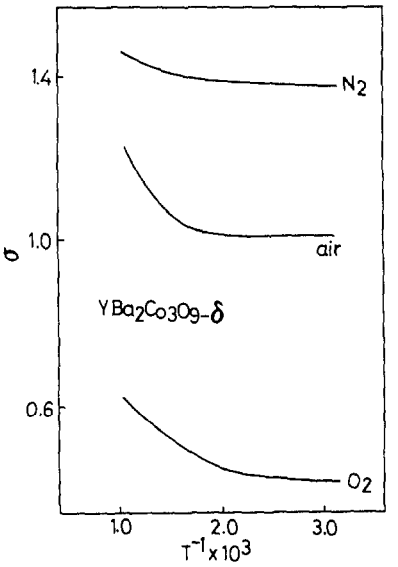

FIG. 8. δ in $YBa_2Co_3O_{9-\delta}$ as a function of temperature in O_2, air, and N_2.

(C in Fig. 7) is a $YBa_2Co_3O_{9-\delta}$ perovskite (cubic, a = 4.14 Å). Consequently, the single phase of $YBa_2Co_3O_{9-\delta}$ perovskite was obtained by the following annealing:

$$\tfrac{1}{2}Y_2O_3 + 2BaCO_3 + \tfrac{3}{2}Co_2O_3 \xrightarrow{1100°C,\ air} Y_2O_3, \text{perovskite, unknown} \xrightarrow{1100°C,\ N_2} \text{perovskite, unknown} \xrightarrow{650°C,\ O_2} YBa_2Co_3O_{9-\delta}\ (\text{perovskite}). \quad (4)$$

Considering that the ionic radii of Co ions are a little smaller than those of Fe ions, the much larger unit cell of $YBa_2Co_3O_{9-\delta}$ (4.14 Å) compared to that of $YBa_2Fe_3O_{9-\delta}$ (about 4.0 Å) is anomalous. Probably, a small amount of Y^{3+} may exist in the Co site.

Figure 8 shows δ in $YBa_2Co_3O_{9-\delta}$ as a function of temperature. Oxygen in the structure releases at temperature higher than about 250°C. Figures 9 and 10 show the temperature dependences of conductivities and Seebeck coefficients, respectively. $YBa_2Co_3O_{9-\delta}$ is also a p-type semiconductor. Since the band structure is not exactly known, the number of electron vacancies, n_1 in Eq. (2), is not presumed. However, the carrier density and the mobility can be estimated by the following equation in a hopping mechanism,

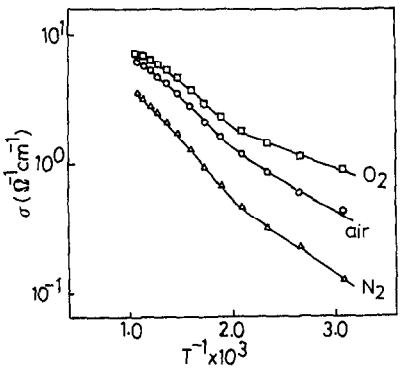

FIG. 9. Conductivity of $YBa_2Co_3O_{9-\delta}$ as a function of temperature in O_2, air, and N_2.

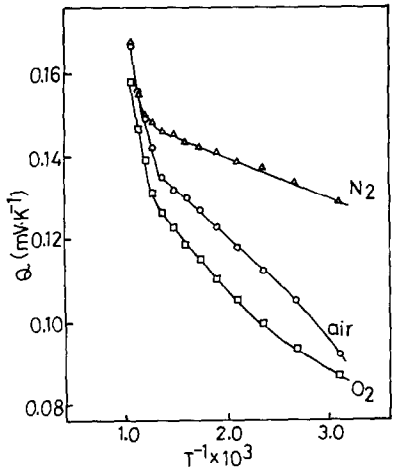

FIG. 10. Seebeck coefficient of $YBa_2Co_3O_{9-\delta}$ as a function of temperature in O_2, air, and N_2.

$$Q = (k/e)\ln(N_p/P), \qquad (5)$$

where N_p is the density of state which is assumed to equal the density of Co ions in the structure ($1.41 \times 10^{22}/cm^3$).

Figure 11 shows the carrier densities and the mobilities estimated by using Eqs. (3) and (5), as a function of temperature. The strong dependences of mobility on temperature indicate that the conduction of $YBa_2Co_3O_{9-\delta}$ is also based on the hopping mechanism. The activation energies of mobility are listed in Table I. The activation energies change at 250°C, where the hopping conduction changes its mechanism. On the other hand, the carrier density decreases strongly at temperatures higher than about 500°C. Probably, two types of oxygen anion will be present in $YBa_2Co_3O_{9-\delta}$ in the temperature range of our measurements. One type, which begins to release from the structure at about 250°C (Fig. 8), will mainly affect the mobility, while the other type, which begins to release at about 500°C, will mainly contribute to the hole density. Figure 12 shows the mobilities and the hole densities as a function of oxygen vacancy at 100 and 200°C. The mobility rather than the hole density is more affected by oxygen vacancy. The mobility decreases with an increase in oxygen vacancy, especially in the range of δ values larger than about one. These results are similar to those for the cases of iron perovskite oxides (6).

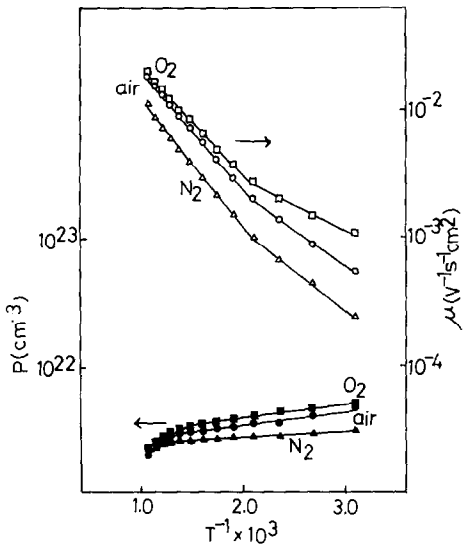

FIG. 11. Hole concentration and mobility of $YBa_2Co_3O_{9-\delta}$ as a function of temperature in O_2, air, and N_2.

Estimation of Band Structure

Table I lists various electrical properties of $YBa_2Fe_3O_{9-\delta}$ and $YBa_2CoO_3O_{9-\delta}$. Carrier densities are almost the same for both oxides, while the mobility of $YBa_2Co_3O_{9-\delta}$ is larger than that of $YBa_2Fe_3O_{9-\delta}$ by about two orders. Considering the unit cell for the former oxide is larger than that for the latter oxide, the above result for mobility seems strange, because the mobility of the carrier in perovskite oxide is primarily determined by overlapping integral between transition metal ions and oxygen ions which increases with a decrease in the distance of *M*–O. Probably, the difference in the mobilities of these oxides will be based on that in the *d* orbitals of

TABLE I

ELECTRICAL PROPERTIES OF $YBa_2Fe_3O_{9-\delta}$ AND $YBa_2Co_3O_{9-\delta}$

Oxide	Conductivity at 100°C ($\Omega^{-1} \cdot cm^{-1}$)	Activation energy of conductivity (eV)	Mobility at 100°C ($V^{-1}\ sec^{-1}\ cm^2$)	Activation energy of mobility (eV)	Hole density at 100°C (cm^{-3})
$YBa_2Fe_3O_{9-\delta}$	4.6×10^{-4} in N_2	0.42 (150–400°C)	5.4×10^{-6}	0.32 (150–400°C)	5.4×10^{20}
$YBa_2Co_3O_{9-\delta}$	1.2 in O_2	0.06 (50–200°C) 0.11 (250–650°C)	1.5×10^{-3}	0.08 (50–200°C) 0.18 (250–650°C)	4.8×10^{21}
	6.1×10^{-1} in air	0.09 (50–200°C) 0.14 (250–650°C)	9.0×10^{-4}	0.11 (50–200°C) 0.18 (250–650°C)	4.1×10^{21}
	2.2×10^{-1} in N_2	0.12 (50–200°C) 0.18 (250–650°C)	4.5×10^{-4}	0.13 (50–200°C) 0.21 (250–650°C)	3.0×10^{21}

Fe and Co ions contributing to the hopping band in the oxide. The d orbital in $YBa_2Fe_3O_{9-\delta}$ contributing the conduction will be t_{2g} and will form the π^*_β hopping band with the P_π orbital of the O^{2-} anion, like the cases of iron perovskite oxides, while that in $YBa_2Co_3O_{9-\delta}$ will be e_g and will form the σ^* hopping band with the P_σ orbital of the O^{2-} anion (7). According to Goodenough (7), the overlapping integral is larger for the σ^* band than for the π^* band. This will be the main reason for the above difference in the mobility for Fe and Co perovskite oxides. Schematic energy diagrams of the band structures of YBa_2-

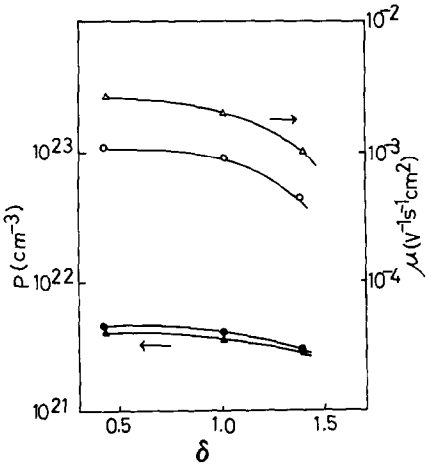

FIG. 12. Hole concentration and mobility of $YBa_2Co_3O_{9-\delta}$ as a function of δ at 100°C (circle symbol) and 200°C (triangle symbol).

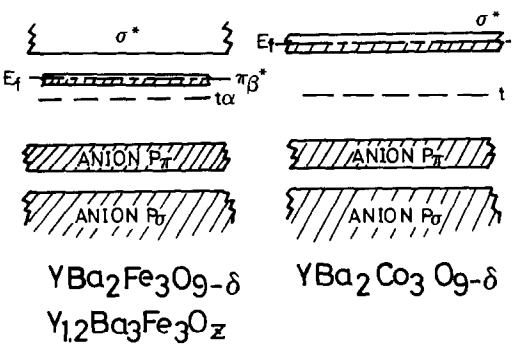

FIG. 13. Band structures of $YBa_2Fe_3O_{9-\delta}$, $Y_{1.2}Ba_3Fe_3O_z$, and $YBa_2Co_3O_{9-\delta}$.

$Fe_3O_{9-\delta}$ and $YBa_2Co_3O_{9-\delta}$ are illustrated in Fig. 13.

References

1. S. B. Oseroff, D. C. Vier, J. F. Smyth, C. T. Salling, S. Schultz, Y. Dalichauch, B. W. Lee, and M. B. Maple, *Solid State Commun.* **64,** 241 (1987).
2. D. Cahen, Z. Moisi, and M. Schwartz, *Mater. Res. Bull.* **22,** 1581 (1987).
3. G. Xiano, F. H. Streiz, A. Gavrin, Y. W. Du, and C. L. Chien, *Phys. Rev. B* **35,** 8782 (1987).
4. E. T. Muromachi, Y. Uchida, and K. Kato, *Jpn. J. Appl. Phys.* **26,** L2087 (1987).
5. S. Geremia, G. Nardin, R. Mosca, L. Randaccio, and E. Zangrando, *Solid State Commun.* **72,** 333 (1989).
6. J. Hombo, Y. Matsumoto, and T. Kawano, *J. Solid State Chem.* **84,** 138 (1990).
7. J. B. Goodenough, *J. Appl. Phys.* **37,** 1415 (1966).